



Size Distributions of Water-Soluble Inorganic Ions in Atmospheric Aerosols During the Meiyu Period in the Yangtze River Delta, China

Zhaoye Wu^{1,2}, Duanyang Liu^{2,3,4*}, Tianliang Zhao¹, Yan Su⁵ and Bin Zhou⁵

¹Key Laboratory for Aerosol-Cloud-Precipitation of China Meteorological Administration, Nanjing University of Information Science and Technology, Nanjing, China, ²Key Laboratory of Transportation Meteorology, CMA, Nanjing, China, ³Nanjing Joint Institute for Atmospheric Sciences, Nanjing, China, ⁴Collaborative Innovation Center of Atmospheric Environment and Equipment Technology, Jiangsu Key Laboratory of Atmospheric Environment Monitoring and Pollution Control (AEMPC), Nanjing University of Information Science and Technology, Nanjing, China, ⁵Wuxi Meteorological Observatory of Jiangsu Province, Wuxi, China

OPEN ACCESS

Edited by:

Lijuan Shen,
University of Toronto, Canada

Reviewed by:

Yi Li,
Intel, United States
Chao Liu,
China Meteorological Administration,
China
Jinhui Gao,
Chengdu University of Information
Technology, China

*Correspondence:

Duanyang Liu
liuduanyang2001@126.com

Specialty section:

This article was submitted to
Atmosphere and Climate,
a section of the journal
Frontiers in Environmental Science

Received: 01 October 2021

Accepted: 21 October 2021

Published: 14 December 2021

Citation:

Wu Z, Liu D, Zhao T, Su Y and Zhou B
(2021) Size Distributions of Water-
Soluble Inorganic Ions in Atmospheric
Aerosols During the Meiyu Period in the
Yangtze River Delta, China.
Front. Environ. Sci. 9:788115.
doi: 10.3389/fenvs.2021.788115

In order to investigate the chemical composition distributions and pollution characteristics of Total water-soluble inorganic ions (TWSII) in the rain period (Meiyu) in the East Asian summer monsoon season, including the impact of Meiyu on air pollution in the Yangtze River Delta, East China, the gaseous pollutant concentrations, the 9 sizes segregated particles, and water-soluble inorganic ions of aerosols were measured on the north shore of Taihu Lake from June 4 to July 5, 2016. Results show that the mass concentrations of atmospheric particulate matters (PM_{2.5} and PM₁₀) and main gaseous pollutants (SO₂, NO₂, CO, and O₃) decrease during the Meiyu period, with the largest decline in PM₁₀ and the smallest in CO. TWSII in atmospheric particles are mainly concentrated in fine particles during the Meiyu period. The values of ρ (TWSII) for PM_{1.1}, PM_{1.1-2.1}, and PM_{2.1-10} before the Meiyu onset are generally greater than those during the Meiyu period. During the first pollution process, the ρ (TWSII) for PM_{1.1} and PM_{1.1-2.1} first increase to the peak values, and then decrease during the moderate rainfall period, when the ρ (TWSII) in PM_{2.1-10} increase to its maximum before the Meiyu onset. The mass concentrations for anions, cations, and total ions at different particle-size sections all exhibit bimodal distributions before and after the Meiyu onset. The mass concentration peaks at a particle size of 1.1–2.1 μm for fine particles, while at 5.8–9.0 μm (before the Meiyu onset) and 9.0–10.0 μm (during the Meiyu period) for coarse particles, respectively. The peak particle size for mass concentration of coarse particles moves toward larger sizes during the Meiyu period. The mass concentrations of SO₄²⁻ at different particle-size sections show a bimodal distribution before the Meiyu onset and a multi-modal distribution during the Meiyu period. The mass concentrations of NO₃⁻ at different particle-size sections show a bimodal distribution before the Meiyu onset and a unimodal distribution during the Meiyu period. The mass concentrations of NH₄⁺ at different particle-size sections present a bimodal distribution before and after the Meiyu onset, with the particle-size for peak concentrations distributing in 1.1–2.1 and 5.8–9.0 μm before the Meiyu onset, and 9.0–10.0 μm during the Meiyu period. The mean value of nitrogen oxidation ratio (NOR) is higher before the Meiyu onset than after, indicating that the

secondary conversion of NO_2 before the Meiyu onset is enhanced. The sulfur oxidation ratio (SOR) values are greater than NOR values, but the concentrations of NO_2 in the same period during the Meiyu period are higher than those of SO_2 , which indicates that the secondary conversion of SO_2 during the Meiyu period on the north bank of Taihu Lake is stronger than that of NO_2 . During the whole observation, the contribution of stationary sources mainly contributed to the atmospheric particulate matters during the Meiyu period. The contributions of vehicle exhaust and coal combustion to fine particles are more obviously affected by the changes in meteorological conditions during the Meiyu period, and the vehicle emissions contribute more to $\text{PM}_{1.1-2.1}$ than to $\text{PM}_{1.1}$.

Keywords: fine particles, meiyu, size distribution, taihu lake, water-soluble inorganic ions, the Yangtze River Delta

INTRODUCTION

In recent years, the negative impact of particulate matter on air quality, climate, and human health in China has attracted more and more public attention (Huang et al., 2018; Zhou et al., 2018; Liu et al., 2019; Zhang et al., 2019; Gu et al., 2020; Gui et al., 2020; Zhang et al., 2020; Wang et al., 2021). Atmospheric particulate matter includes primary particulate matter and secondary particulate matter (Dai et al., 2013; Wang S. et al., 2019). Primary particulate matter is usually produced by direct emissions of pollutant sources, such as soil dust from the ground, roads, and construction sites, biomass burning, and sea salt particles transported from the ocean. The secondary particulate matter is generally formed by the oxidation reaction of SO_2 (sulfur dioxide), NO_x (nitrogen dioxide), NH_3 (ammonia), and other gases (Yao et al., 2020).

Long-term exposure to fine particulate matter ($\text{PM}_{2.5}$) is one of the risk factors for excess deaths in China, with heavy smog significantly increasing the risk of acute death among residents (Wang et al., 2015, 2020). Previous studies have found that WSII accounts for 30–80% of urban particulate matter (Shen, et al., 2009; Tan, et al., 2009; Wang et al., 2015). It can be seen that WSII is an important component of particulate matter, and the study of characteristic changes of WSII helps us to have a deeper understanding of the physical and chemical properties, sources, and formation mechanism of particulate matter (Guo et al., 2020; Wang et al., 2019 b). Some studies have found that there are significant seasonal differences in WSII concentration (Qiao et al., 2015). Gao, et al. (2016) found that NO_3^- , SO_4^{2-} , and NH_4^+ (SNA) in WSII were characteristic ions of secondary pollution. The proportion of SNA mass concentration in $\text{PM}_{2.5}$ ranges from 20 to 70%, and even exceeds 70% (He et al., 2017). Guo et al. (2010) and Zhang et al. (2018) studied that the ion mass concentration spectrum can be used to investigate the formation mechanism of WSII. Some studies have found that the concentration of NO_3^- and SO_4^{2-} in droplet modes increases significantly in the process of pollution, and their peak particle sizes move towards larger particle sizes (Sun et al., 2013; Tian et al., 2016).

Located on the north bank of Taihu Lake, Wuxi is one of the central cities in the Yangtze River Delta region with a dense population, large industrial volume, and a high level of urbanization. With the rapid development of the regional

economy, a large amount of energy consumption and the continuous growth of motor vehicle ownership, the air quality of Wuxi presents complex air pollution dominated by $\text{PM}_{2.5}$, PM_{10} , O_3 , and NO_2 (Guo et al., 2013). Meiyu in Jianghuai Region is an important weather phenomenon in eastern China, and the meiyu rainy season precipitation is a product of interactions between the East Asian summer monsoon system and the Eurasian mid-high-latitude circulation (Xia et al., 2021). Due to the prevailing wind direction and precipitation in the monsoon climate, the air quality in Wuxi is relatively clean in summer compared with winter. However, in the summer harvest and planting stage in June, the particulate matter emitted from straw burning will lead to haze pollution events in Wuxi (Guo et al., 2013; Wang et al., 2021).

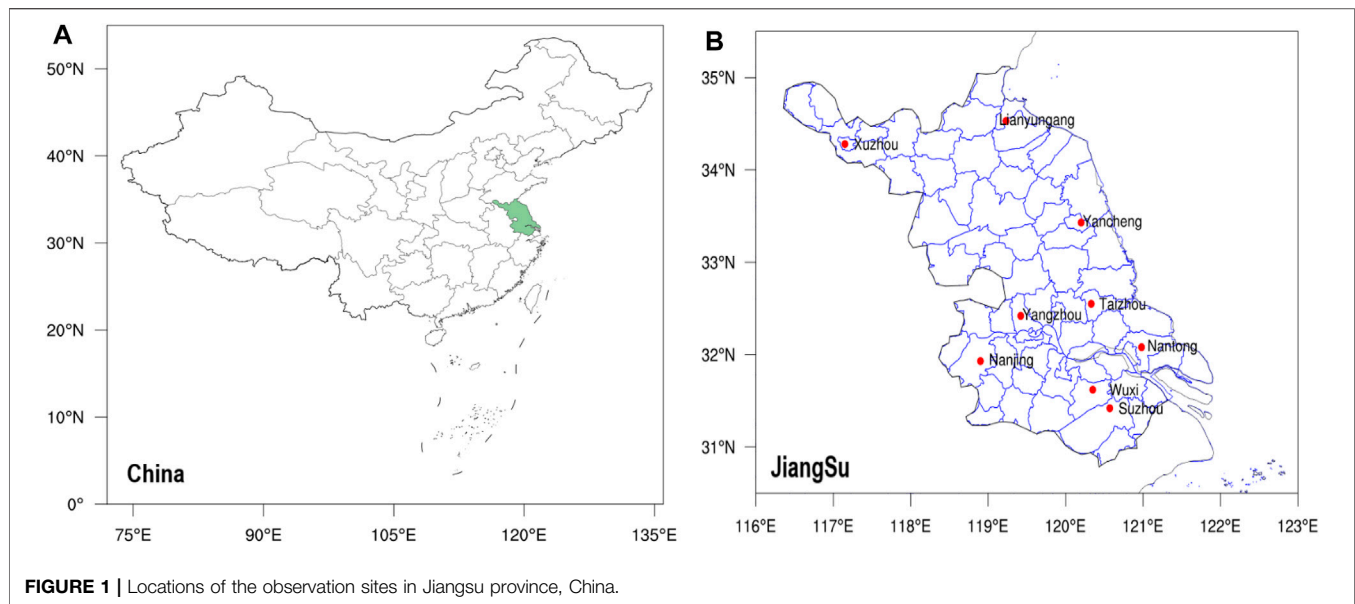
In this study, we collected size-segregated aerosol samples in Wuxi during an intensive sampling campaign from June to July 2016. The primary motivation of this study is to determine the chemical composition distributions and pollution characteristics of the TWSII species in the nine size segregated particles in the season changing period, including evolution in the components and particle size changes in the pollution process. Furthermore, the correlation of sulfur and nitrogen oxidation rates with the meteorological conditions were investigated to clarify the dominant meteorological factors affecting the secondary formation of sulfate and nitrate in different size fractions. The results would improve our understanding of the secondary formation of haze pollutions in the economically developed area during the Meiyu period and can also provide insight for the investigation of the human health effects of urban particulate matter in different sizes.

First, the instruments, experiments, data, and analysis methods are described in *Experiments and Data*. We analyze the meteorological conditions pollutions features, spectral distribution, and ionic species of aerosol in *Results and discussion*. Concluding is made in *Conclusion*.

EXPERIMENTS AND DATA

Observation Stations and Experiment Descriptions

Wuxi is located in the middle of the Yangtze River Delta, on the northern shore of Taihu Lake. In this study, we selected Wuxi



meteorological observational station (WMOS, 31.6127°N, 120.3544°E, altitude: 3.2 m) as the sampling site (**Figure 1**). All the measurements were conducted on June 4 to July 5, 2016 (Guo et al., 2013; Liu et al., 2018). The monitoring site is surrounded by farms and is located on the ground. Thus, the observations at this site could help further understand the atmospheric pollution condition in the Yangtze River Delta Cities Group Area (YRDCGA) and the influences from the inland or upwind polluted areas and the Taihu Lake in a regional air quality perspective.

Water-Soluble Inorganic Ions

The observation of aerosol particles was conducted by using a 9-stage Anderson-type aerosol sampler (Anderson 2000 Inc., United States). 31 batches of aerosol samples were gathered across the Meiyu period in Wuxi. The sampling was conducted on the Meteorological observation field. 24 h size-fractionated PM samples were taken continuously for 1 month (begin at 8:00 am the first day and end at 08:00 the next day) at the flow rate of 28.3 L/min. The particle size range of the nine stages are <0.43, 0.43–0.65, 0.65–1.1, 1.1–2.1, 2.1–3.3, 3.3–4.7, 4.7–5.8, 5.8–9.0, and 9.0–10.0 μm for water-soluble ionic components.

The sampling instrument was using the 80 mm Teflon filter (Whatman, Clifton, England) for water-soluble inorganic ionic components, and the membranes were weighted by Mettler Toledo MX-5 microbalance after constant temperature (25°C) and humidity (50%) treatment for 48 h before and after sampling, the microbalance was calibrated using standard weight. The weight difference before and after sampling is particle weight (Wang et al., 2015; Liu et al., 2018).

The 850 professional Ion Chromatography (IC) (Metrohm, Switzerland) was used to analyze the water-soluble inorganic ions, NO_3^- , SO_4^{2-} , NH_4^+ , Ca^{2+} , Mg^{2+} , Na^+ , K^+ , Cl^- , F^- , and NO_2^- were measured. Chromatography includes a conductivity

detector, column oven, with an 858 auto-injector, and MagIC Net chromatography workstation (Metrohm, Switzerland); Detailed information can be referred to Wang et al. (2015).

Meteorological and Pollutant Data

In this study, monitoring instruments (Thermo-Fisher Scientific, United States) were selected to analyze gaseous pollutants, including CO (48i), NO_2 (42i), O_3 (49i), and SO_2 (43i), and the particulate matters, including PM_{10} and $\text{PM}_{2.5}$ during the sampling times. The meteorological parameters, including relative humidity (RH), pressure, vapor pressure, precipitation, dew point temperature (Td), temperature (T), visibility, wind direction (WD), and wind speed (WS). All the data were obtained hourly from the Wuxi meteorological observational station (MOS) worked synchronously on the observation site.

Meiyu in 2016

Meiyu (rainy period of East Asian monsoon season) is a weather phenomenon with regional and temporal characteristics in the middle and lower reaches of the Yangtze River in China (Xiang et al., 2016). It is the product of the transition season of east Asian atmospheric circulation from spring to summer. There is always a persistent precipitation stage of Meiyu from June to July every year, which is called Meiyu period for the middle and lower reaches of the Yangtze River. During the Meiyu periods, precipitation shows obvious interannual variabilities (Xia et al., 2021).

Based on the observation of the Meiyu period lasting from June 19, 2016, to July 11 on the north bank of Taihu Lake, the periods from June 4, 2016, to June 18, 2016, and from June 19, 2016, to July 5, 2016, are defined respectively before and after the onset of Meiyu in this study. The total precipitation during the Meiyu period is 404.5 mm, which is much greater than that (105.4 mm) before the Meiyu onset.

TABLE 1 | Statistic of meteorological conditions during sampling time.

	Before the meiyu period			During the meiyu period			The observation period		
	Min	Max	Mean	Min	Max	Mean	Min	Max	Mean
T (°C)	19.9	32.8	24.6	19.5	33.0	25.7	18.7	33.0	25.2
T _d (°C)	17.0	24.8	21.2	17.5	28.2	23.9	16.4	28.2	22.7
Surface pressure (hPa)	998.7	1010.7	1006.3	999.4	1012.4	1006.3	998.7	38.2	1006.3
Surface vapor pressure (hPa)	19.4	31.4	25.3	20.0	38.2	29.8	18.6	1012.4	27.7
RH (%)	45.0	100.0	82.9	51.0	100.0	90.7	45.0	100.0	87.2
Wind speed (m/s)	0.2	6.1	2.1	0.0	6.0	1.0	0.0	6.1	2.0
Total precipitation (mm)		105.4			404.5			509.9	

RESULTS AND DISCUSSION

Pollutant Concentrations and Meteorological Conditions During the Meiyu Period

Meteorological Conditions

The changes of meteorological conditions on the north bank of Taihu Lake during the observation period are shown in **Table 1** and **Figure 2**. The surface pressure, wind speed, and temperature change little around the onset of Meiyu. During the observation period, the average wind speed maintains about 2.0 m s⁻¹, while the air temperature keeps in the range of 19.0°C–33.0°C with an average of 25.2°C. The frequency and amount of precipitation increase significantly after the Meiyu onset, with the precipitation increasing from 105.4 mm (from June 4 to June 18) to 404.5 mm (from June 19 to July 11). The precipitation increase leads to significant increases in surface water-vapor pressure, relative humidity, and dew-point temperature. Specifically, the average surface water-vapor pressure is 25.3 hPa before the Meiyu onset, which is significantly lower than that (29.8 hPa) during the Meiyu period. The average dew-point temperatures (relative humidity) before and after the onset of Meiyu are 21.2 and 23.9°C (82.9 and 90.7%), respectively. Comparatively, the relative humidity after the onset of Meiyu is closer to saturation than before. Moreover, the wind direction changes obviously and frequently during the Meiyu period on the north bank of Taihu Lake.

Concentration Variations of PM_{2.5}, PM₁₀, and Gaseous Pollutants

Table 2 shows the daily mean concentrations of PM_{2.5}, PM₁₀, and main gaseous pollutants before and after the onset of Meiyu. The mass concentrations of five main air pollutants after the onset of Meiyu significantly decrease due to the rainfall influence. Specifically, the mass concentrations of PM₁₀ and PM_{2.5} are 65.36 and 50.20 μg m⁻³ before the onset of Meiyu, which respectively drop to 38.27 and 29.05 μg m⁻³ after the Meiyu onset. For gaseous pollutants, the mass concentrations of SO₂, NO₂, and O₃ decrease from 12.10, 51.77, and 77.83 μg m⁻³ to 7.91, 41.51, and 51.89 μg m⁻³, respectively.

Before the Meiyu onset, the north bank of Taihu Lake experienced two pollution processes. The first process lasted from 0800 Beijing Time (BJT) on June 6 to 2000 BJT on June 9, and the second process lasted from 2000 BJT on June 12 to 2000

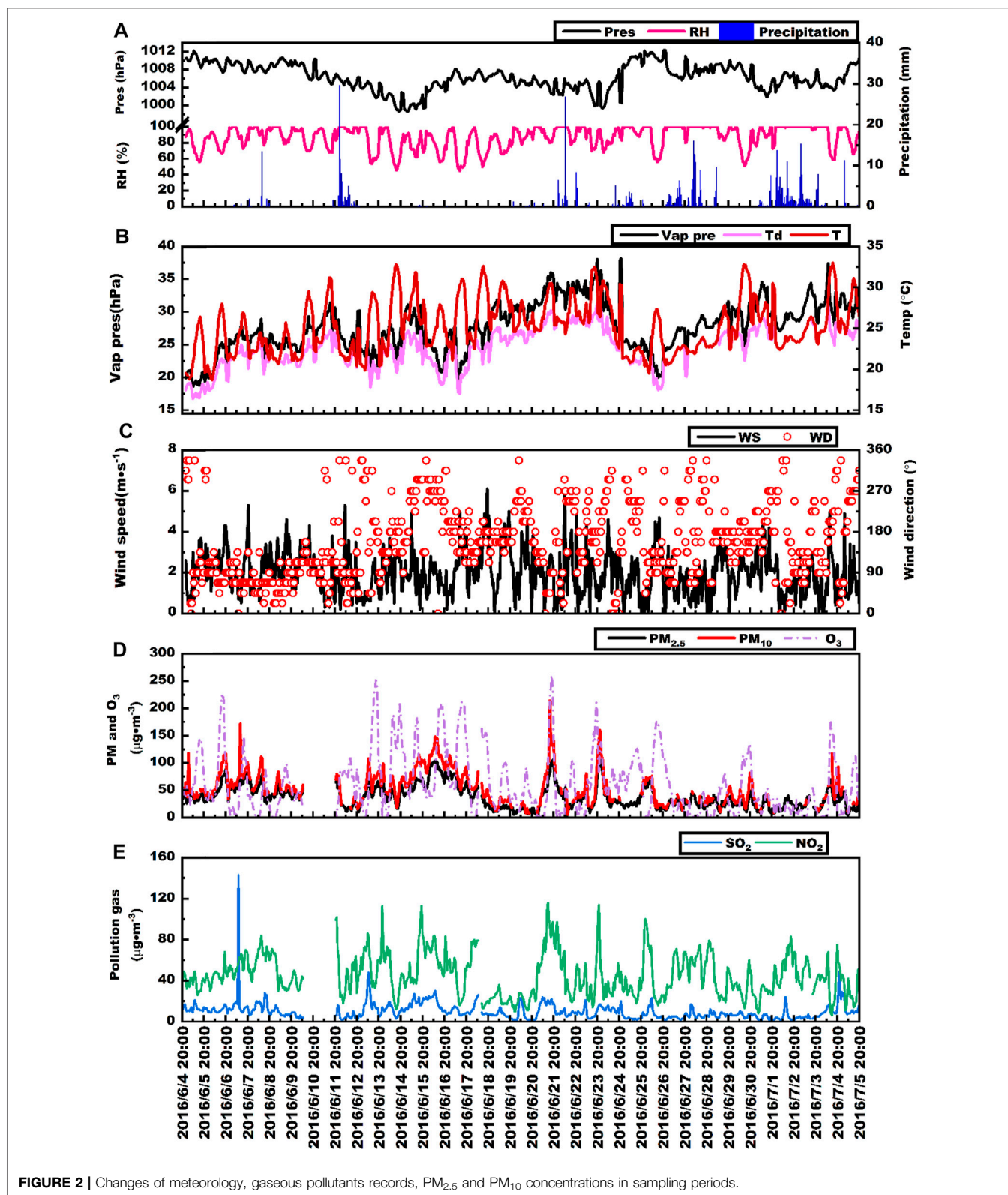
BJT on June 18. The mass concentrations of PM_{2.5} and PM₁₀ peaked at 112 and 172 μg m⁻³ in the first process, and peaked at 103 and 148 μg m⁻³ during the second process (**Figures 2D,E**). Although the pollution process during the Meiyu period is not as long as that before the Meiyu onset, the mass concentrations of air pollutants during this period also experienced short fluctuations, where the mass concentrations of PM_{2.5} reached 106 and 120 μg m⁻³ at 2000 BJT on June 21 and 2300 BJT on June 23, respectively (**Figures 2D,E**). According to the hourly precipitation (**Figure 2**) in the Meiyu period, these two fluctuations occurred during the intermittent period of precipitation. While the mass concentrations of air pollutants were significantly lower during other periods, which maintained below 30 μg m⁻³ for PM_{2.5}. The precipitation increase and changeable wind direction could be the reasons for the decline of air pollutants.

Changes of Water-Soluble Inorganic Ions in Atmospheric Aerosols

Differences of Water-Soluble Inorganic Ions Before and After the Onset of Meiyu

Table 3 depicts the differences between the concentrations of water-soluble inorganic ions before and after the onset of Meiyu. The average concentration of total water-soluble inorganic ions (ρ(TWSII)) in PM₁₀ is (28.59 ± 7.27) μg m⁻³, while the average ρ(TWSII) in PM_{1.1}, PM_{1.1–2.1} and PM_{2.1–10} are (11.22 ± 3.90) μg m⁻³ (5.18 ± 2.77) μg m⁻³ and (12.19 ± 2.89) μg m⁻³, respectively. Before the onset of Meiyu, the average ρ(TWSII) in PM_{1.1}, PM_{1.1–2.1} and PM_{2.1–10} are 13.36 ± 4.84, 6.55 ± 3.46, and 12.3 ± 3.46 μg m⁻³, and they are 9.34 ± 3.72, 3.98 ± 2.19, and 12.10 ± 5.3 μg m⁻³ after the onset of Meiyu, with the ρ(TWSII) decreasing by 30, 39 and 2%, respectively. The values of ρ(TWSII) in fine and coarse particles before the Meiyu onset are higher than those during the Meiyu period.

As shown in **Figure 3A**, the total proportions of four major water-soluble inorganic ions (NH₄⁺, Ca²⁺, SO₄²⁻ and NO₃⁻) in PM_{1.1} and PM_{1.1–2.1} are 82 and 87%, respectively. The major water-soluble inorganic ions for PM_{2.1–10} are Ca²⁺, NH₄⁺, SO₄²⁻ and Na⁺, accounting for 72% of the total. The anion with the largest proportion in PM_{1.1}, PM_{1.1–2.1}, and PM_{2.1–10} is SO₄²⁻. Besides, the cation with the largest proportion in PM_{1.1} and PM_{1.1–2.1} is NH₄⁺, but it is Ca²⁺ in PM_{2.1–10}. It indicates that NH₄⁺ mainly exists in fine particles, while Ca²⁺ mainly in coarse



particles. Furthermore, the concentration of NH_4^+ decreases with the increase of particle size before and after the onset of Meiyu (Figure 3B).

The concentrations of NH_4^+ , Ca^{2+} , SO_4^{2-} and NO_3^- rank top four in submicron particles, fine particles, or coarse particles before the Meiyu onset (Table 3 and Figure 3). The average

TABLE 2 | The daily average concentration of PM_{2.5}, PM₁₀, and gaseous pollutants before and during the Meiyu period.

	Before the meiyu period			During the meiyu period		
	Min	Max	Mean	Min	Max	Mean
PM _{2.5} (μg/m ³)	23.79	84.67	50.20	12.21	52.88	29.05
PM ₁₀ (μg/m ³)	30.13	111.71	65.36	16.17	81.10	38.27
SO ₂ (μg/m ³)	4.90	18.46	12.10	3.67	15.71	7.91
NO ₂ (μg/m ³)	37.75	90.33	51.77	20.58	73.38	41.51
O ₃ (μg/m ³)	12.33	133.67	77.83	15.14	101.87	51.89

concentrations of ten kinds of ions in PM_{1.1} are in decreasing order of NH₄⁺>SO₄²⁻>Ca²⁺>NO₃⁻>Na⁺>K⁺>Mg²⁺>Cl⁻>F⁻>NO₂⁻, while those in PM_{1.1-2.1} follow the order of NH₄⁺>SO₄²⁻>NO₃⁻>Ca²⁺>Na⁺>K⁺>Mg²⁺>Cl⁻>F⁻>NO₂⁻. For PM_{2.1-10}, the average concentrations are in order of Ca²⁺>NH₄⁺>SO₄²⁻>Na⁺>NO₃⁻>Mg²⁺>K⁺>Cl⁻>F⁻>NO₂⁻.

The concentrations of NH₄⁺, Ca²⁺, SO₄²⁻ and NO₃⁻ are still the highest four after the Meiyu onset, with slight changes in the concentrations of different ions. The concentration of Ca²⁺ increases after the Meiyu onset, which is related to the road construction around the observation site (Wang et al., 2021). The concentrations of NH₄⁺, SO₄²⁻ and NO₃⁻ decrease significantly, while the concentrations of Na⁺, K⁺, Mg²⁺, Cl⁻, F⁻ and NO₂⁻ change little. During the Meiyu period, the average concentrations of ten kinds of ions follow the order of NH₄⁺>Ca²⁺>SO₄²⁻>NO₃⁻>Na⁺>K⁺>Mg²⁺>Cl⁻>F⁻>NO₂⁻ in PM_{1.1}, the order of NH₄⁺>Ca²⁺>NO₃⁻>SO₄²⁻>Na⁺>K⁺>Mg²⁺>Cl⁻>F⁻>NO₂⁻ in PM_{1.1-2.1}, and the order of Ca²⁺>NH₄⁺>SO₄²⁻>Na⁺>NO₃⁻>Mg²⁺>K⁺>Cl⁻>F⁻>NO₂⁻ in PM_{2.1-10}.

Compositions of Water-Soluble Inorganic Ions in PM_{1.1}, PM_{1.1-2.1} and PM_{2.1-10}

The changes of the mass concentrations of water-soluble inorganic ions in PM_{1.1}, PM_{1.1-2.1}, and PM_{2.1-10} with time during the Meiyu period on the north bank of Taihu Lake are depicted in **Figure 4**. The ρ(TWSII) in PM_{1.1}, PM_{1.1-2.1}, and PM_{2.1-10} before the Meiyu onset are generally greater than those during the Meiyu period, but there are some differences in the concentration changes. The ρ(TWSII) in PM_{1.1-2.1} changes most

obviously before and after the Meiyu onset, followed by PM_{1.1}, while the ρ(TWSII) changes little in PM_{2.1-10}. This indicates the effect of frequent precipitation during the Meiyu period on the removal of PM_{1.1}, PM_{1.1-2.1}, and PM_{2.1-10}, especially for PM_{1.1-2.1}.

Figure 4 also shows that the changes of ρ(TWSII) in PM_{1.1}, PM_{1.1-2.1}, and PM_{2.1-10} with time are generally consistent, but there are some differences in some periods. During June 18–20, 2016, the ρ(TWSII) in PM_{1.1} decreased first and then increased, while the change of ρ(TWSII) in PM_{2.1-10} was opposite, and the ρ(TWSII) in PM_{1.1-2.1} presented a consistent increase. Besides, the concentrations varied little in fine particles but changes drastically for coarse particles. This changing trend may be related to the compositions and formation mechanisms of water-soluble inorganic ions of different sizes.

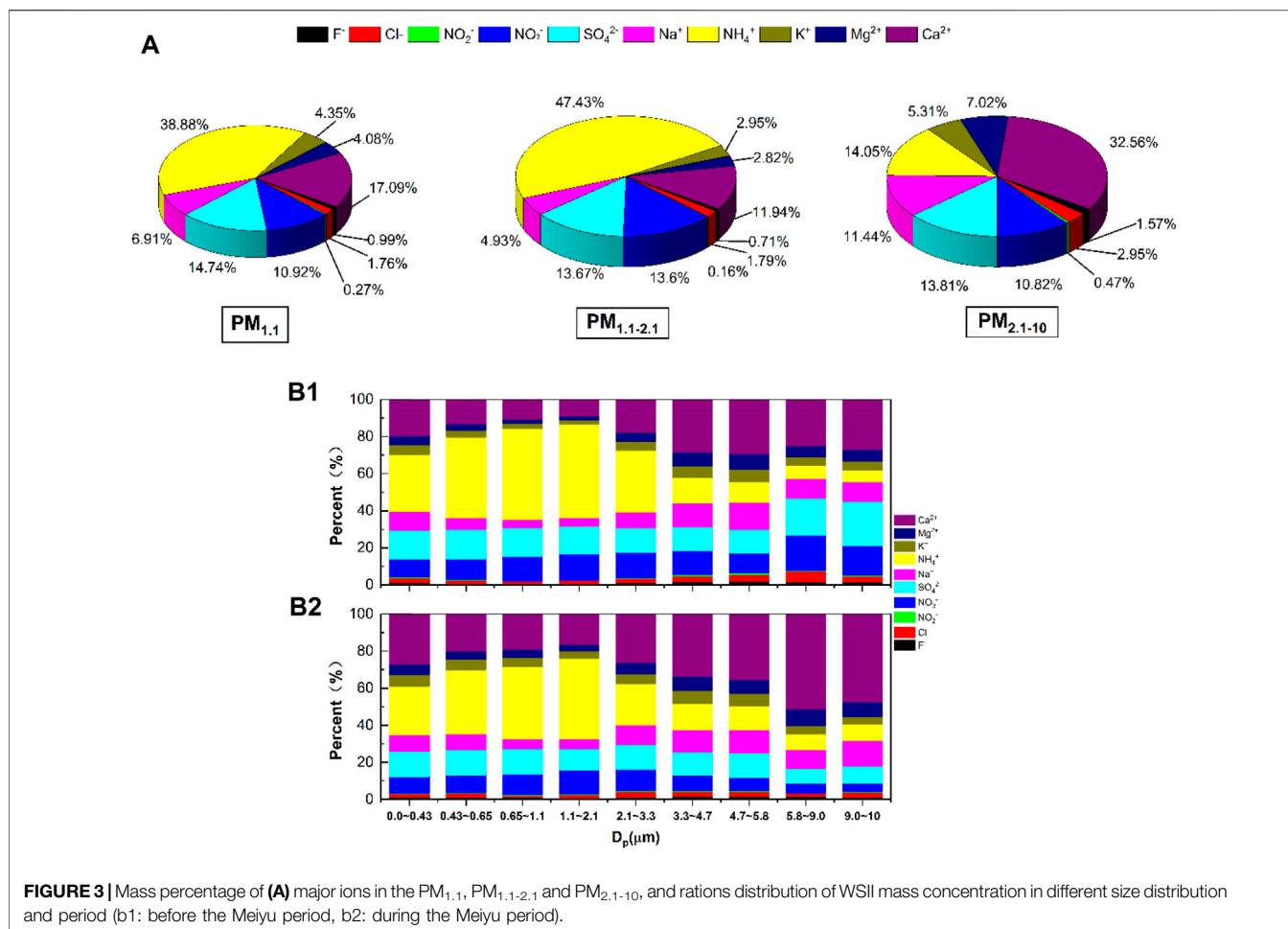
Corresponding to the pollution processes mentioned in *Concentration variations of PM2.5, PM10, and gaseous pollutants*, the ρ(TWSII) in PM_{1.1} and PM_{1.1-2.1} increased obviously from June 5 to June 7 before the Meiyu onset, and the ρ(TWSII) in PM_{1.1} and PM_{1.1-2.1} decreased from June 7 to June 8, while the ρ(TWSII) in PM_{2.1-10} increased to a maximum value before the Meiyu onset. From June 14 to June 16, the ρ(TWSII) in PM_{1.1} and PM_{1.1-2.1} increased to their maximums of 21.34 and 12.05 μg m⁻³ during the observation period, respectively. Meanwhile, the ρ(TWSII) of PM_{2.1-10} decreased from June 14 to June 15 and increased from June 15 to June 16.

During the first process of air pollution (from 0800 BJT on June 6 to 2000 BJT on June 9) before the Meiyu onset, the mass concentrations of NH₄⁺, SO₄²⁻ and NO₃⁻ in PM_{1.1}, PM_{1.1-2.1} and PM_{2.1-10} increased, especially the concentrations of NH₄⁺ in PM_{1.1} and PM_{1.1-2.1}. During the second process (from 2000 BJT on June 12 to 2000 BJT on June 18), the concentrations of NH₄⁺, SO₄²⁻ and NO₃⁻ in PM_{1.1} and PM_{1.1-2.1} increased, while the concentrations of these ions in PM_{2.1-10} had no change, which is different from those in the first process. What is the reason for this?

Moreover, the two short fluctuations at 2000 BJT on June 21 and 2300 BJT on June 23 are only reflected as the increases in the concentrations of NH₄⁺, SO₄²⁻ and NO₃⁻ in PM_{1.1} and PM_{1.1-2.1}. The above four fluctuations may be related to the change of SO₂ concentration before and after the Meiyu onset. On the one hand,

TABLE 3 | The average concentrations (μg/m³) of WSII in particulate matters before and during the Meiyu period.

	Before the meiyu period			During the meiyu period		
	PM _{1.1}	PM _{1.1-2.1}	PM _{2.1-10}	PM _{1.1}	PM _{1.1-2.1}	PM _{2.1-10}
NH ₄ ⁺	5.74 ± 2.64	3.30 ± 2.13	1.86 ± 2.13	3.16 ± 1.79	1.72 ± 1.29	1.59 ± 0.63
Ca ²⁺	1.79 ± 0.37	0.58 ± 0.09	3.05 ± 0.09	2.03 ± 0.49	0.65 ± 0.14	4.77 ± 2.93
SO ₄ ²⁻	2.10 ± 0.67	0.99 ± 0.50	2.08 ± 0.50	1.26 ± 0.41	0.46 ± 0.21	1.33 ± 0.41
NO ₃ ⁻	1.56 ± 0.67	0.92 ± 0.54	1.82 ± 0.54	0.93 ± 0.53	0.51 ± 0.37	0.88 ± 0.30
Na ⁺	0.85 ± 0.19	0.30 ± 0.09	1.36 ± 0.09	0.71 ± 0.20	0.22 ± 0.08	1.43 ± 0.51
K ⁺	0.47 ± 0.12	0.15 ± 0.03	0.64 ± 0.03	0.50 ± 0.12	0.16 ± 0.03	0.66 ± 0.08
Mg ²⁺	0.46 ± 0.05	0.15 ± 0.02	0.78 ± 0.02	0.45 ± 0.07	0.14 ± 0.02	0.92 ± 0.26
Cl ⁻	0.23 ± 0.10	0.12 ± 0.06	0.43 ± 0.06	0.17 ± 0.09	0.07 ± 0.04	0.30 ± 0.16
F ⁻	0.11 ± 0.02	0.04 ± 0.00	0.20 ± 0.00	0.11 ± 0.01	0.04 ± 0.01	0.18 ± 0.01
NO ₂ ⁻	0.03 ± 0.01	0.01 ± 0.00	0.08 ± 0.00	0.03 ± 0.01	0.01 ± 0.00	0.04 ± 0.01
TWSII	13.36 ± 4.84	6.55 ± 3.46	12.30 ± 3.46	9.34 ± 3.72	3.98 ± 2.19	12.10 ± 5.30



the increase of SO₄²⁻ concentration in PM_{1.1-2.1} during the Meiyu period is due to the gas-to-particle conversion of smaller particles; on the other hand, the SO₄²⁻ converts to larger-size particles.

Spectrum Distribution of Mass Concentrations of TWSII

The particle-size distribution of water-soluble ions can characterize the source and formation mechanism of ions (Zhang et al., 2018). **Figure 5A** indicates that the mass concentration spectrums of total anions, total cations, and total ions within different particle-size sections present bimodal distributions before and after the Meiyu onset. The mass concentrations of fine particles peak at the particle-size of 1.1–2.1 μm, while the mass concentrations of coarse particles respectively peak at particle-size of 5.8–9.0 and 9.0–10.0 μm before and after the Meiyu onset, indicating that the particle-size corresponding to peak concentrations in coarse particles moves toward the larger particle sizes after the Meiyu onset. The variation characteristics for mass concentrations of anions, cations, and total ions are similar during the observation period, with the ions mainly concentrating in the section of fine particles. The peak concentration of ions in fine particles

before the Meiyu onset is higher than that during the Meiyu period. While in coarse particles, the peak concentration of anions before the Meiyu onset is higher. Meanwhile, the peak concentrations of total cations and total ions before the Meiyu onset are lower than those during the Meiyu period.

Figure 6 displays the variations of the particle-size distributions of total anions, total cations, and total ions in water-soluble inorganic ions overtime during the observation. Before June 19, 2016, the total anions, total cations, and total ions in fine particles grew rapidly and reached their peak concentrations. During June 8–15 before the Meiyu onset, the concentration of total anions with the particle sizes of 4.5– and 0.65–1.1 μm in coarse particles increased more rapidly than those in other particle sizes (**Figure 6A**). The particle sizes for the peak of mass concentrations of total ions in coarse particles moved toward larger particle sizes after the Meiyu onset. The period with an increasing concentration for total anions with the particle size of 9–10 μm in coarse particles accounted for 47% of the total Meiyu period, while the concentration of the total anions at the particle size of 5.8–9.0 μm decreased during the same period. Meanwhile, the environmental relative humidity was greater than 90% (**Figure 2C**), indicating an obvious effect of the hygroscopic growth of the total anions in coarse particles. As shown in

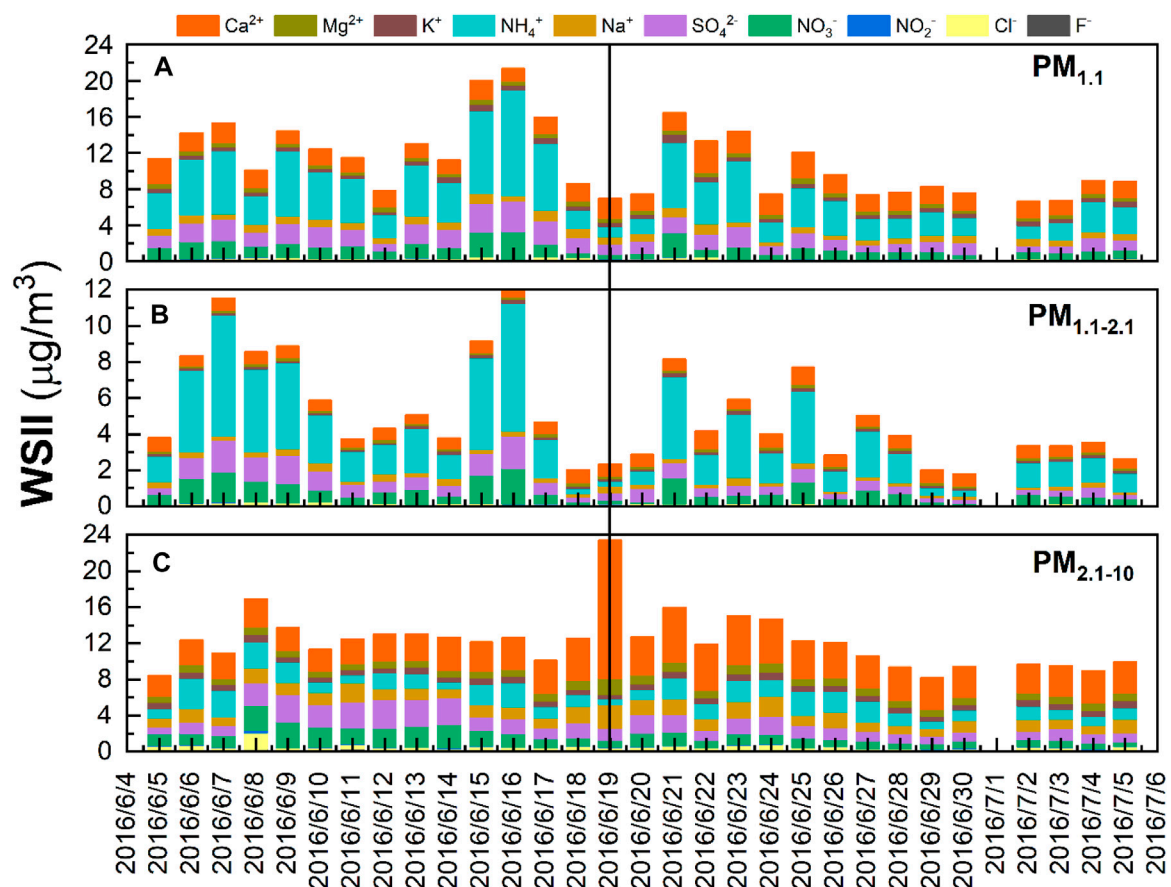
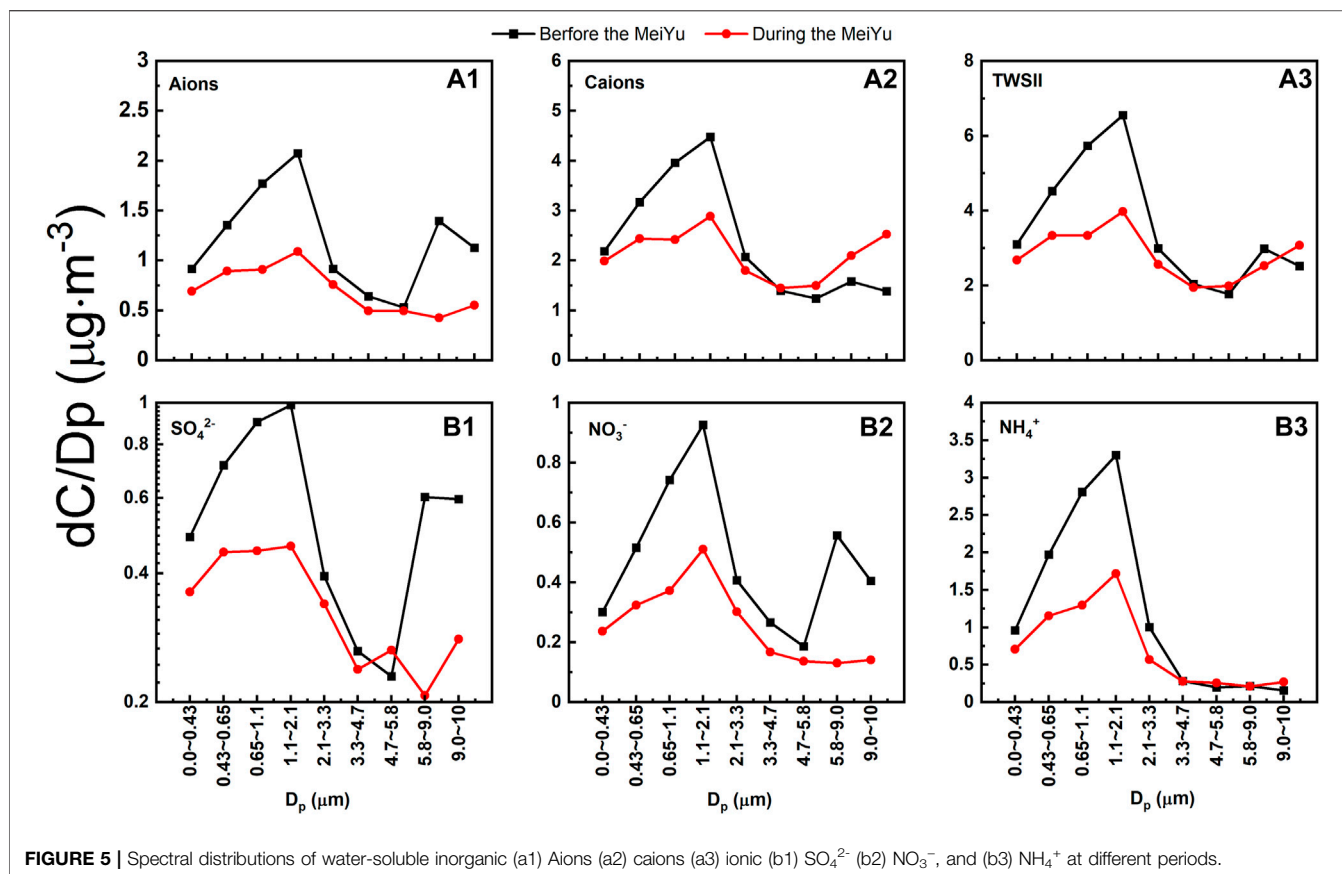


FIGURE 4 | Time series of major inorganic ions in (A) $PM_{1.1}$, (B) $PM_{1.1-2.1}$, (C) $PM_{2.1-10}$ during the sampling period.

Figure 6B, the concentrations of total cations and total ions in coarse particles during the Meiyu period were higher than those before the Meiyu onset, with the maximum concentrations of total cations and total ions in coarse particles being 0.81 (0.95) and $3.28 \mu\text{g m}^{-3}$ ($10.56 \mu\text{g m}^{-3}$) before (after) the Meiyu onset, respectively. The maximum concentration during the Meiyu period was 3.2 times that before the Meiyu onset. The main reason for the sharp increase in the peak concentration during the Meiyu period was that the concentrations of the cations at 5.8–9.0 and 9.0–10.0 μm increased sharply on June 19, and the changes of total cation concentrations in coarse particles were roughly the same on both June 18 and June 19, indicating the same source for the total cations on June 18 and 19. **Figure 2** shows that the winds on June 18 and 19 were both southerly, and the daily means of temperature, relative humidity, and surface wind speed were 27.6°C (28.4°C), 75.6% (77.9%), and 3.0 m s^{-1} (2.6 m s^{-1}) on June 18 (June 19), indicating no significant changes in meteorological elements. While the local anthropogenic emissions near the observation site have a more obvious effect on the concentration of total cations than meteorological factors do. During the observation period, the particle size of total ions has a more consistent distribution with that of total cations than total anions. It indicates that the cations in water-soluble inorganic ions in atmospheric particulate matters on the north

bank of Taihu Lake played an important role in the chemical composition of ions during the Meiyu period in 2016 (Wang et al., 2021).

The particle-size distribution characteristics of different ions and their sources are further analyzed, with the size distributions of each ion before and after the Meiyu onset shown in **Figure 7**, and the time series for different particle-size distributions shown in **Figure 5B**. The particle size of SO_4^{2-} shows a bimodal distribution before the Meiyu onset and a multi-modal distribution during the Meiyu period. Before the Meiyu onset, the mass concentration of SO_4^{2-} peaks at a particle size of 1.1–2.1 μm in fine particles, while at 5.8–9.0 μm in coarse particles. After the Meiyu onset, the mass concentration of SO_4^{2-} presents a bimodal distribution with its peaks at particle-size of 0.43–0.65 μm and 1.1–2.1 μm in fine particles, and particle-size of 4.7–5.8 and 9.0–10.0 μm in coarse particles. As indicated in the sequence variation (**Figure 7**), before the Meiyu onset, the mass concentration of SO_4^{2-} in fine particles peaks at particle-size of 0.43–2.1 μm and the proportions for the frequencies in three different particle-size sections are 36, 21, and 43%, respectively. During the Meiyu period, the mass concentration of SO_4^{2-} in fine particles peaks at particle-size of 0–2.1 μm , and the proportions for the frequencies in different particle sizes are 19, 25, 6, and 40%, respectively. It indicates that



SO_4^{2-} in fine particles is mainly generated by the reactions in the cloud and the gas-phase reaction. While the two reactions during the Meiyu period are weaker than those before the Meiyu onset. The particle size for the peak concentration of SO_4^{2-} in coarse particles moves toward larger particle sizes during the Meiyu period. This may be related to higher environmental humidity during the Meiyu period, resulting in the hygroscopic growth of sulfates in coarse particles.

The mass concentration of NO_3^- at different particle-size sections shows a bimodal distribution before the Meiyu onset, and a unimodal distribution after the Meiyu onset. The mass concentration of NO_3^- in fine particles peaks at particle-size of 1.1–2.1 μm , while at 5.8–9.0 μm in coarse particles. **Figure 5B** shows that before the Meiyu onset, the mass concentration of NO_3^- in fine particles peaks at particle-size of 0.43–2.1 μm , with the proportions of frequencies for particle-size in four particle-size sections accounting for 13, 25, 6, and 56%, respectively. The effect of gas-phase conversion (liquid-phase reaction) during Meiyu is stronger (weaker) than that before Meiyu. Before the Meiyu onset, the mass concentration of NO_3^- in coarse particles peaks at particle-size of 2.1–3.3 and 5.8–10.0 μm , and the proportions of frequencies for particle-size within the three particle-size sections account for 36, 57, and 7%, respectively. The peak particle-size of NO_3^- distributes in all five particle-size sections of 2.1–10 μm after the Meiyu onset, with the proportions of frequencies accounting for 50, 6, 6, 13, and 25%, respectively. It

can be concluded that the sources of NO_3^- in coarse particles after the Meiyu onset are more complex than before. The proportion for NO_3^- having particle-size within 5.8–9.0 μm decreases significantly, which may be attributed to the removal effect of increasing rainfall during the Meiyu period. The concentration of NH_4^+ at different particle-size sections presents a bimodal distribution before and unimodal distribution during the Meiyu, with the particle-size of peak concentration distributing in 1.1–2.1 and 5.8–9.0 μm (before the Meiyu), and 9.0–10.0 μm (during the Meiyu). NH_4^+ is mainly found in fine particles, with the mass fraction accounting for 79.2% (**Figure 5B**).

Changes of Secondary Aerosols

The sulfur oxidation ratio (SOR) and nitrogen oxidation ratio (NOR) are often used to characterize the conversion degree of SO_2 and NO_2 to SO_4^{2-} and NO_3^- , respectively ($\text{SOR} = [\text{SO}_4^{2-}]/([\text{SO}_4^{2-}] + [\text{SO}_2])$, $\text{NOR} = [\text{NO}_3^-]/([\text{NO}_3^-] + [\text{NO}_2])$, where the $[\text{SO}_4^{2-}]$, $[\text{SO}_2]$, $[\text{NO}_3^-]$, and $[\text{NO}_2]$ are the molar concentrations ($\mu\text{mol m}^{-3}$) in the particulate matters and gas phase.) (Guo et al., 2020). Higher SOR or NOR values indicate that more secondary aerosol particulates are converted from SO_2 and NO_2 (Liu et al., 2016; Wang et al., 2019a,b). It has been found that when the SOR and NOR values are greater than 0.1, the photochemical reaction occurs in the atmosphere (Ohta and Okita 1990). **Figure 8** shows the time series for the NOR, SOR, and concentrations of SO_2 , NO_2 , SO_4^{2-} and NO_3^-

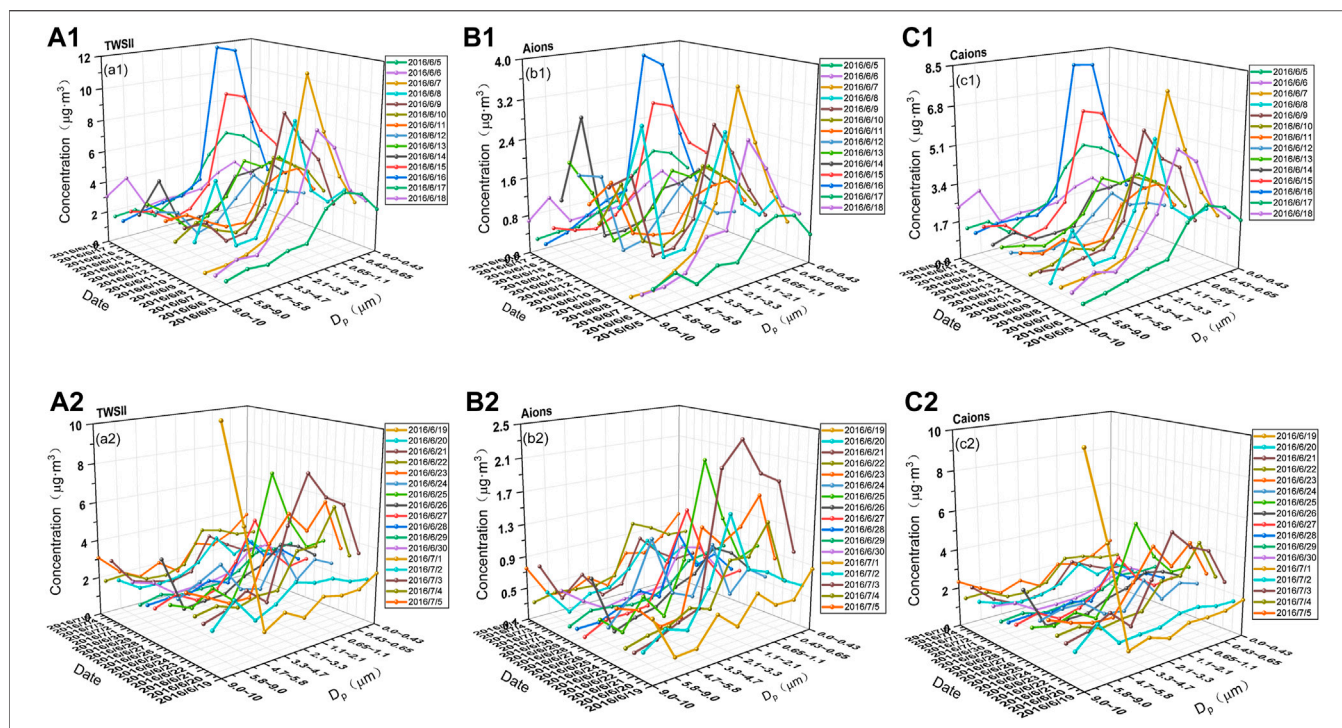


FIGURE 6 | Daily variations in spectral distribution of water-soluble inorganic (a1, a2) ionic (b1, b2) aions and (c1, c2) caions at different period (a1, b1, c1) before the Meiyu period and (a2, b2, c2) during the Meiyu period.

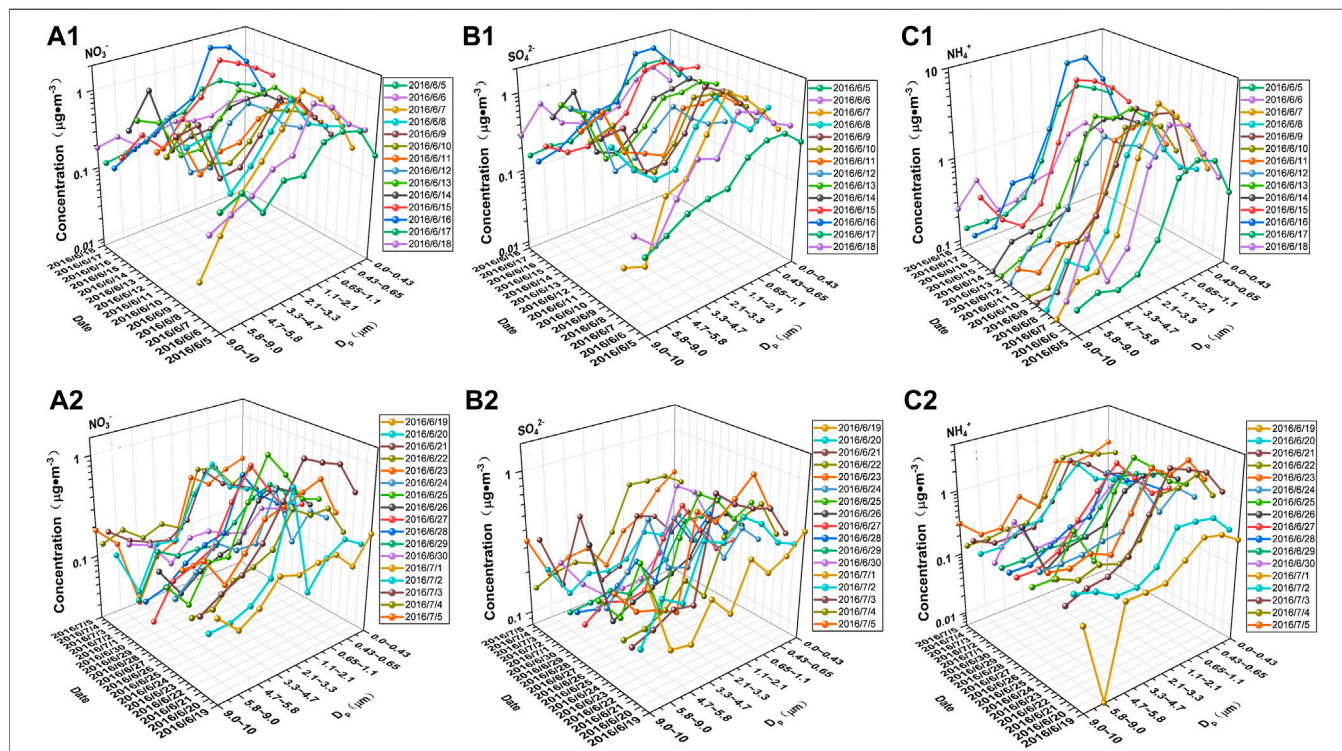


FIGURE 7 | Daily variations in spectral distribution of water-soluble inorganic (a1, a2) NO_3^- (b1, b2) SO_4^{2-} and (c1, c2) NH_4^+ at different period.

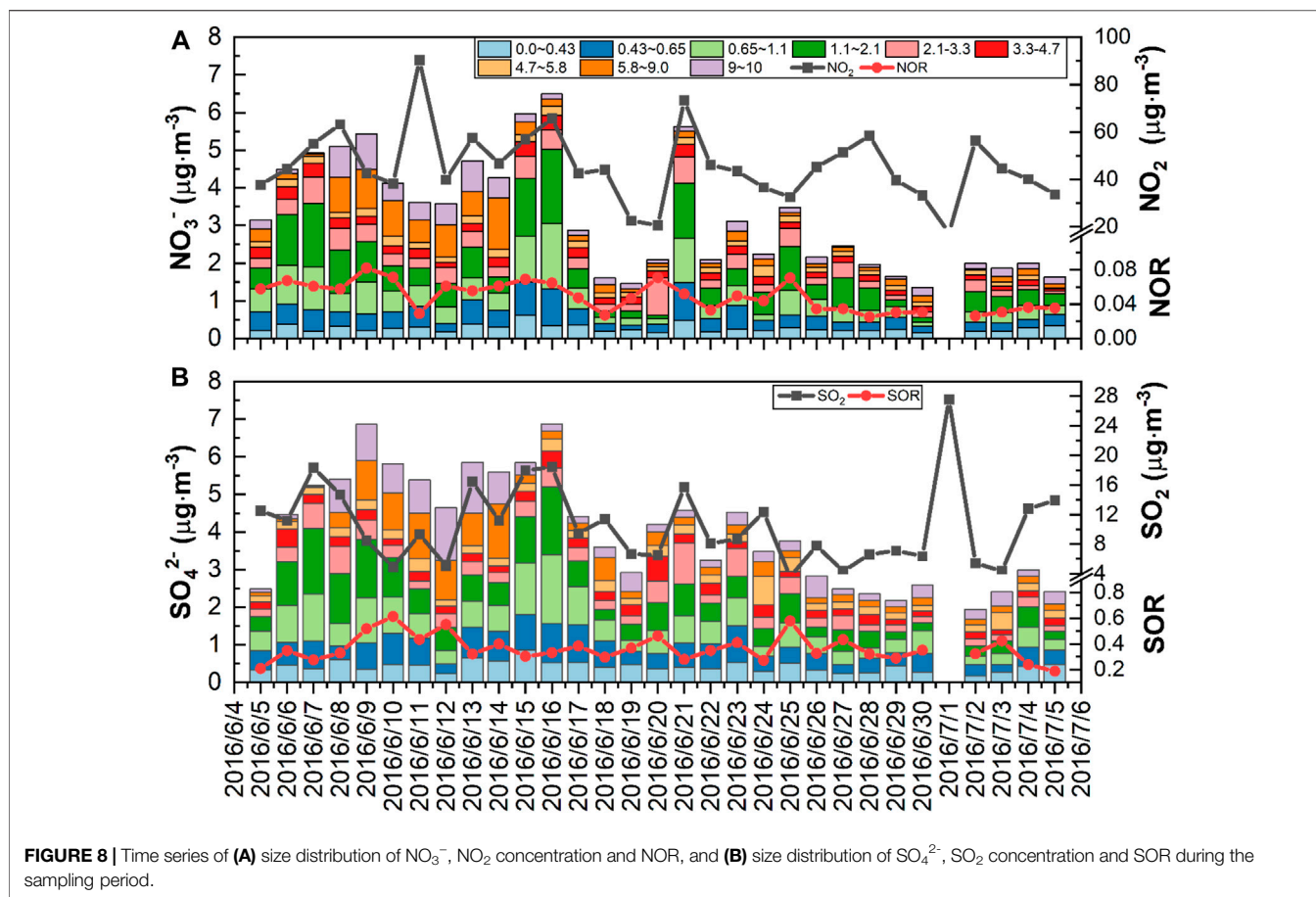


TABLE 4 | Correlation coefficient of NOR and SOR between O_3 concentrations, Temperature, Relative humidity and Precipitation in particulate matters.

	O_3	T	RH	Precipitation
$\text{SOR}_{\text{PM}_{1,1}}$	0.12	-0.13	0.01	-0.11
$\text{SOR}_{\text{PM}_{1,1-2.1}}$	-0.07	-0.51 ^a	0.33	0.07
$\text{SOR}_{\text{PM}_{2,1-10}}$	-0.19	-0.28	0.35	0.28
$\text{NOR}_{\text{PM}_{1,1}}$	0.58 ^a	-0.11	-0.33	-0.49 ^b
$\text{NOR}_{\text{PM}_{1,1-2.1}}$	0.34	-0.44 ^b	0.05	-0.13
$\text{NOR}_{\text{PM}_{2,1-10}}$	0.15	-0.14	-0.10	-0.25

^aCorrelation is significant at the 0.01 level.

^bCorrelation is significant at the 0.05 level.

during the Meiyu period on the north bank of Taihu Lake. It can be found that the NOR values during the observation are below 0.1, and the average NOR value before the Meiyu onset is higher, indicating that the secondary conversion of NO_2 before the Meiyu onset is greater than after.

Table 4 shows the correlation coefficients of the SOR and NOR with O_3 , temperature, relative humidity, and daily precipitation in different particle-size sections. It can be seen that the NOR in $\text{PM}_{1,1}$ is positively correlated with the O_3 concentration ($R_2 = 0.58$) and negatively correlated with the daily precipitation ($R_2 = -0.49$), indicating that the O_3 concentration has a more obvious impact on the NOR in

$\text{PM}_{1,1}$. The NOR in $\text{PM}_{1,1-2.1}$ is negatively correlated with the temperature, where high-temperature results in disassociation of and volatilization of NH_4NO_3 to form gaseous HNO_3 (Zhao et al., 2018). As the average temperature during the Meiyu period is higher than that before the Meiyu onset, the NOR decreases during the Meiyu period.

During the Meiyu period, the SOR values in $\text{PM}_{2,1-10}$ are all above 0.1, the SOR values in $\text{PM}_{1,1}$ are generally above 0.1 in most periods, while the SOR values in $\text{PM}_{1,1-2.1}$ are the smallest among the three particle-size sections. For $\text{PM}_{1,1}$, $\text{PM}_{1,1-2.1}$ and $\text{PM}_{2,1-10}$, the SOR values are greater than the NOR values, but the concentration of NO_2 in the same period during the Meiyu period is higher than that of SO_2 , indicating that the secondary conversion of SO_2 during the Meiyu period on the north bank of Taihu Lake is stronger than that of NO_2 .

The mass ratio of $\text{NO}_3^-/\text{SO}_4^{2-}$ can be used to qualitatively analyze the relative importance of mobile sources (vehicle exhaust) and stationary sources (coal combustion) to particulate matters of sulfur and nitrogen in the atmosphere. A higher ratio indicates the predominance of mobile sources over stationary sources of pollutants (Chang et al., 2015). Figure 9 shows that the mass ratios of $\text{NO}_3^-/\text{SO}_4^{2-}$ in $\text{PM}_{1,1}$, $\text{PM}_{1,1-2.1}$ and $\text{PM}_{2,1-10}$ before the Meiyu onset range in 0.13–0.38 (the mean ratio is 0.29), 0.22–0.55 (the mean ratio is 0.36) and 0.21–0.67 (the mean ratio is 0.36), respectively. While during the Meiyu period, the

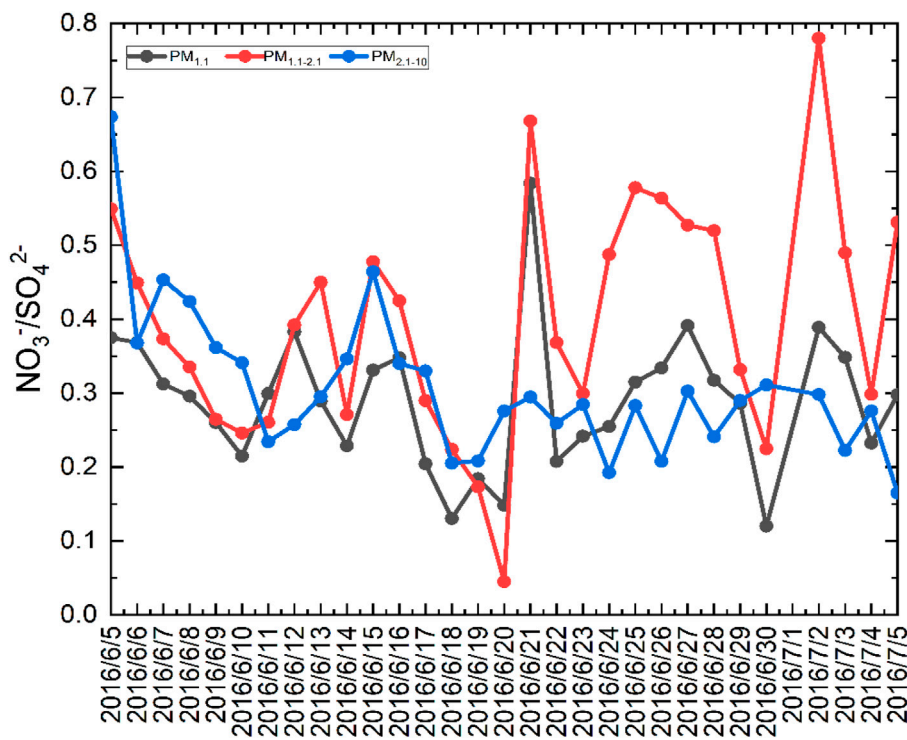


FIGURE 9 | Time series of $\text{NO}_3^-/\text{SO}_4^{2-}$ in $\text{PM}_{1.1}$, $\text{PM}_{1.1-2.1}$, $\text{PM}_{2.1-10}$ during the sampling time.

mass ratios of $\text{NO}_3^-/\text{SO}_4^{2-}$ in $\text{PM}_{1.1}$, $\text{PM}_{1.1-2.1}$ and $\text{PM}_{2.1-10}$ range in 0.12–0.58 (the mean ratio is 0.29), 0.05–0.78 (the mean ratio is 0.43) and 0.17–0.31 (the mean ratio is 0.26), respectively. The mass ratios of $\text{NO}_3^-/\text{SO}_4^{2-}$ during the whole observation period are less than 0.80, indicating that compared with mobile sources, the stationary sources contribute more to the relative contribution of atmospheric particulate matter on the north bank of Taihu Lake.

The variation ranges for the mass ratio of $\text{NO}_3^-/\text{SO}_4^{2-}$ before the Meiyu onset are smaller than those during the Meiyu period in $\text{PM}_{1.1}$ and $\text{PM}_{1.1-2.1}$, while the situation is quite the reverse in $\text{PM}_{2.1-10}$. It indicates that the contributions of vehicle exhaust and coal combustion to fine particles are more obviously affected by the changes in meteorological conditions during the Meiyu period. **Figure 9** reveals that the mean ratio of $\text{NO}_3^-/\text{SO}_4^{2-}$ in $\text{PM}_{1.1-2.1}$ before Meiyu onset is smaller than that during the Meiyu period, and it is higher than that in $\text{PM}_{1.1}$, indicating that the vehicle emissions contribute more to $\text{PM}_{1.1-2.1}$ than to $\text{PM}_{1.1}$. Moreover, the contribution of vehicle exhaust increases during the Meiyu period, which is the same as the result from a case study in Wuxi in 2014 (Liu et al., 2018).

CONCLUSION

In order to investigate the chemical composition distributions and the impact of Meiyu on air pollution in the Yangtze River Delta, East China, the gaseous pollutant concentrations, the nine sizes segregated particles, and water-soluble inorganic ions of

aerosols were measured on the north shore of Taihu Lake from June 4 to July 5, 2016. This observational study is concluded as follows:

The mass concentrations of atmospheric particulate matters ($\text{PM}_{2.5}$ and PM_{10}) and main gaseous pollutants (SO_2 , NO_2 , CO , and O_3) decrease during the Meiyu period, with the largest decline in PM_{10} and the smallest in CO , which could be regulated by meteorological changes before and after Meiyu onset. Water-soluble inorganic ions in atmospheric particles are mainly concentrated in fine particles during the Meiyu period on the north bank of Taihu Lake. The values of $\rho(\text{TWSII})$ for $\text{PM}_{1.1}$, $\text{PM}_{1.1-2.1}$, and $\text{PM}_{2.1-10}$ before the Meiyu onset are generally greater than those during the Meiyu period. During the first pollution process, the $\rho(\text{TWSII})$ for $\text{PM}_{1.1}$ and $\text{PM}_{1.1-2.1}$ first increase to the peak values, and then decrease during the moderate rainfall period, when the $\rho(\text{TWSII})$ in $\text{PM}_{2.1-10}$ increase to its maximum before the Meiyu onset.

The mass concentrations for anions, cations, and total ions at different particle-size sections all exhibit bimodal distributions before and after the Meiyu onset. The mass concentration peaks at a particle size of 1.1–2.1 μm for fine particles, while at 5.8–9.0 μm (before the Meiyu onset) and 9.0–10.0 μm (during the Meiyu period) for coarse particles, respectively. The peak particle size for mass concentration of coarse particles moves toward larger particle sizes during the Meiyu period. The mass concentrations of SO_4^{2-} at different particle-size sections show a bimodal distribution before the Meiyu onset and a multi-modal distribution during the Meiyu period. The mass concentrations of

NO₃⁻ at different particle-size sections show a bimodal distribution before the Meiyu onset and a unimodal distribution during the Meiyu period. The mass concentrations of NH₄⁺ at different particle-size sections present a bimodal distribution before and after the Meiyu onset, with the particle-size for peak concentrations distributing in 1.1–2.1 and 5.8–9.0 μm before the Meiyu onset, and 9.0–10.0 μm during the Meiyu period.

The mean value of NOR is higher before the Meiyu onset than after, indicating that the secondary conversion of NO₂ before the Meiyu onset is greater. The SOR values are greater than NOR values, but the concentrations of NO₂ in the same period during the Meiyu period are higher than those of SO₂, which indicates that the secondary conversion of SO₂ during the Meiyu period on the north bank of Taihu Lake is stronger than that of NO₂. During the whole observation, the relative contribution of stationary sources to atmospheric particulate matter on the north bank of Taihu Lake is more than the relative contribution of mobile sources. The contributions of vehicle exhaust and coal combustion to fine particles are more obviously affected by the changes in meteorological conditions during the Meiyu period, and the vehicle emissions contribute more to PM_{1,1–2,1} than to PM_{1,1}.

As the crop residue burning ban was issued in 2015, the air quality before and after the Meiyu has improved a lot, further studies are needed to determine the effect of meiyu on the removal of air pollutants.

REFERENCES

- Chang, Q., Yang, F., Li, X., Cao, Y., Wang, H., and Tian, M. (2015). Characteristics of Mass and Chemical Species Size Distributions of Particulate Matter during Haze Pollution in the winter in Beijing. *Acta Scientiae Circumstantiae* 35, 363–370. (In Chinese).
- Dai, W., Gao, J., Cao, G., and Ouyang, F. (2013). Chemical Composition and Source Identification of PM_{2.5} in the Suburb of Shenzhen, China. *Atmos. Res.* 122, 391–400. doi:10.1016/j.atmosres.2012.12.004
- Gao, J., Peng, X., Chen, G., Xu, J., Shi, G.-L., Zhang, Y.-C., et al. (2016). Insights into the Chemical Characterization and Sources of PM_{2.5} in Beijing at a 1-h Time Resolution. *Sci. Total Environ.* 542, 162–171. doi:10.1016/j.scitotenv.2015.10.082
- Gu, P., Qian, J., Liu, D., Wang, K., Dai, Z., Peng, X., et al. (2020). Cold Fronts Transport Features of North China Pollutant over Jiangsu Province, China. *Atmos. Pollut. Res.* 11 (10), 1785–1796. doi:10.1016/j.apr.2020.07.015
- Gui, K., Che, H., Zeng, Z., Wang, Y., Zhai, S., Wang, Z., et al. (2020). Construction of a Virtual PM_{2.5} Observation Network in China Based on High-Density Surface Meteorological Observations Using the Extreme Gradient Boosting Model. *Environ. Int.* 141, 105801. doi:10.1016/j.envint.2020.105801
- Guo, H., Simpson, I. J., Ding, A. J., Wang, T., Saunders, S. M., Wang, T. J., et al. (2010). Carbonyl Sulfide, Dimethyl Sulfide and Carbon Disulfide in the Pearl River Delta of Southern China: Impact of Anthropogenic and Biogenic Sources. *Atmos. Environ.* 44 (31), 3805–3813. doi:10.1016/j.atmosenv.2010.06.040
- Guo, W., Zhang, Z., Zheng, N., Luo, L., Xiao, H., and Xiao, H. (2020). Chemical Characterization and Source Analysis of Water-Soluble Inorganic Ions in PM_{2.5} from a Plateau City of Kunming at Different Seasons. *Atmos. Res.* 234, 104687. doi:10.1016/j.atmosres.2019.104687
- Guo, Y. F., Liu, D. Y., Zhou, B., Xia, J., Wu, Y., and Hu, Y. H. (2013). Study on Haze Characteristics in Wuxi and its Impact Factors. *Meteorol. Monthly* 39, 1314–1324. (in Chinese).
- He, J., Gong, S., Yu, Y., Yu, L., Wu, L., Mao, H., et al. (2017). Air Pollution Characteristics and Their Relation to Meteorological Conditions during 2014–

DATA AVAILABILITY STATEMENT

The raw data supporting the conclusions of this article will be made available by the authors, without undue reservation.

AUTHOR CONTRIBUTIONS

Author Contributions: Conceptualization, DL; methodology, TZ; software, ZW and BZ; validation, DL; formal analysis, ZW; investigation, ZW and YS; resources, DL, and YS; data curation, ZW and BZ; writing—original draft preparation, DL and ZW; writing—review and editing, DL and TZ; visualization, ZW and BZ; supervision, DL and ZW; project administration, DL; funding acquisition, DL.

FUNDING

This work was jointly supported by the National Key Research and Development Program of China (No. 2019YFC0214604), the Postgraduate Research and Practice Innovation Program of Jiangsu Province (Grant Nos. KYCX21_0972), the National Natural Science Foundation of China (42075063), Open fund by Jiangsu Key Laboratory of Atmospheric Environment Monitoring and Pollution Control (KHK 2005), and the Jiangsu Meteorological Bureau General project (KZ201902).

2015 in Major Chinese Cities. *Environ. Pollut.* 223, 484–496. doi:10.1016/j.envpol.2017.01.050

- Huang, X., Wang, Z., and Ding, A. (2018). Impact of Aerosol-PBL Interaction on Haze Pollution: Multiyear Observational Evidences in North China. *Geophys. Res. Lett.* 45 (16), 8596–8603. doi:10.1029/2018gl079239
- Liu, C., Hua, C., Zhang, H., Zhang, B., Wang, G., Zhu, W., et al. (2019). A Severe Fog-Haze Episode in Beijing-Tianjin-Hebei Region: Characteristics, Sources and Impacts of Boundary Layer Structure. *Atmos. Pollut. Res.* 10 (4), 1190–1202. doi:10.1016/j.apr.2019.02.002
- Liu, D., Su, Y., Peng, H., Yan, W., Li, Y., Liu, X., et al. (2018). Size Distributions of Water-Soluble Inorganic Ions in Atmospheric Aerosols during the Meiyu Period on the North Shore of Taihu Lake, China. *Aerosol Air Qual. Res.* 18, 2997–3008. doi:10.4209/aaqr.2018.04.0123
- Liu, Z., Hu, B., Zhang, J., Yu, Y., and Wang, Y. (2016). Characteristics of Aerosol Size Distributions and Chemical Compositions during Wintertime Pollution Episodes in Beijing. *Atmos. Res.* 168, 1–12. doi:10.1016/j.atmosres.2015.08.013
- Ohta, S., and Okita, T. (1990). A Chemical Characterization of Atmospheric Aerosol in Sapporo. *Atmos. Environ. A. Gen. Top.* 24, 815–822. doi:10.1016/0960-1686(90)90282-r
- Qiao, T., Zhao, M., Xiu, G., and Yu, J. (2015). Seasonal Variations of Water Soluble Composition (WSOC, Hulis and WSIs) in PM₁ and its Implications on Haze Pollution in Urban Shanghai, China. *Atmos. Environ.* 123, 306–314. doi:10.1016/j.atmosenv.2015.03.010
- Shen, Z., Cao, J., Arimoto, R., Han, Z., Zhang, R., Han, Y., et al. (2009). Ionic Composition of TSP and PM_{2.5} during Dust Storms and Air Pollution Episodes at Xi'an, China. *Atmos. Environ.* 43 (18), 2911–2918. doi:10.1016/j.atmosenv.2009.03.005
- Sun, Y., Wang, Z., Fu, P., Jiang, Q., Yang, T., Li, J., et al. (2013). The Impact of Relative Humidity on Aerosol Composition and Evolution Processes during Wintertime in Beijing, China. *Atmos. Environ.* 77, 927–934. doi:10.1016/j.atmosenv.2013.06.019
- Tan, J.-H., Duan, J.-C., Chen, D.-H., Wang, X.-H., Guo, S.-J., Bi, X.-H., et al. (2009). Chemical Characteristics of Haze during Summer and winter in Guangzhou. *Atmos. Res.* 94 (2), 238–245. doi:10.1016/j.atmosres.2009.05.016

- Tian, S. L., Pan, Y. P., and Wang, Y. S. (2016). Size-resolved Source Apportionment of Particulate Matter in Urban Beijing during Haze and Non-haze Episodes. *Atmos. Chem. Phys.* 16 (1), 1–19. doi:10.5194/acp-16-1-2016
- Wang, B., Luo, X., Liu*, D., Su, Y., and Wu, Z. (2021). The Effect of Construction Dust and Agricultural Fertilization on the Precipitation Chemical Composition during Summer in the Yangtze River Delta Area, China. *Atmos. Pollut. Res.* 12 (7), 101121. doi:10.1016/j.apr.2021.101121
- Wang, H., Zhu, B., Shen, L., Xu, H., An, J., Xue, G., et al. (2015). Water-soluble Ions in Atmospheric Aerosols Measured in Five Sites in the Yangtze River Delta, China: Size-Fractionated, Seasonal Variations and Sources. *Atmos. Environ.* 123, 370–379. Part B. doi:10.1016/j.atmosenv.2015.05.070
- Wang, S., Yin, S., Zhang, R., Yang, L., Zhao, Q., Zhang, L., et al. (2019a). Insight into the Formation of Secondary Inorganic Aerosol Based on High-Time-Resolution Data during Haze Episodes and Snowfall Periods in Zhengzhou, China. *Sci. Total Environ.* 660, 47–56. doi:10.1016/j.scitotenv.2018.12.465
- Wang, X., Wei, W., Cheng, S., Yao, S., Zhang, H., and Zhang, C. (2019b). Characteristics of PM_{2.5} and SNA Components and Meteorological Factors Impact on Air Pollution through 2013–2017 in Beijing, China. *Atmos. Pollut. Res.* 10, 1976–1984. doi:10.1016/j.apr.2019.09.004
- Wang, Y., Wild, O., Chen, H., Gao, M., Wu, Q., Qi, Y., et al. (2020). Acute and Chronic Health Impacts of PM_{2.5} in China and the Influence of Interannual Meteorological Variability. *Atmos. Environ.* 229, 117397. doi:10.1016/j.atmosenv.2020.117397
- Xia, Y., Qian, H., Yao, S., and Sun, T. (2021). Multiscale Causes of Persistent Heavy Rainfall in the Meiyu Period over the Middle and Lower Reaches of the Yangtze River. *Front. Earth Sci.* 9, 700878. doi:10.3389/feart.2021.700878
- Xiang, Y., Lu, P., Cheng, T., Xie, Z., and Wang, W. (2016). Evolution Characteristics of the Jiangsu Plum Rain in Recent 54 Years and its Monitoring Analysis in 2014. *J. Meteorol. Sci.* 36 (5), 681–688. (In Chinese).
- Yao, Q., Liu, Z., Han, S., Cai, Z., Liu, J., Hao, T., et al. (2020). Seasonal Variation and Secondary Formation of Size-Segregated Aerosol Water-Soluble Inorganic Ions in a Coast Megacity of North China Plain. *Environ. Sci. Pollut. Res. Int.* 27 (21), 26750–26762. doi:10.1007/s11356-020-09052-0
- Zhang, J., Tong, L., Huang, Z., Zhang, H., He, M., Dai, X., et al. (2018). Seasonal Variation and Size Distributions of Water-Soluble Inorganic Ions and Carbonaceous Aerosols at a Coastal Site in Ningbo, China. *Sci. Total Environ.* 639, 793–803. doi:10.1016/j.scitotenv.2018.05.183
- Zhang, L., Guo, X., Zhao, T., Gong, S., Xu, X., Li, Y., et al. (2019). A Modelling Study of the Terrain Effects on Haze Pollution in the Sichuan Basin. *Atmos. Environ.* 196, 77–85. doi:10.1016/j.atmosenv.2018.10.007
- Zhang, W., Wang, H., Zhang, X., Peng, Y., Zhong, J., Wang, Y., et al. (2020). Evaluating the Contributions of Changed Meteorological Conditions and Emission to Substantial Reductions of PM_{2.5} Concentration from winter 2016 to 2017 in Central and Eastern China. *Sci. Total Environ.* 716, 136892. doi:10.1016/j.scitotenv.2020.136892
- Zhao, Q. Y., Jiang, N., Yan, Q. S., Wang, S. B., Han, S. J., Yang, L. M., et al. (2018). Size Distribution Characteristics of Water-Soluble Inorganic Ions during Summer and Autumn in Zhengzhou. *Huan Jing Ke Xue* 39, 4866–4875. (In Chinese). doi:10.13227/j.hj.kx.201803102
- Zhou, D., Ding, K., Huang, X., Liu, L., Liu, Q., Xu, Z., et al. (2018). Transport, Mixing and Feedback of Dust, Biomass Burning and Anthropogenic Pollutants in Eastern Asia: a Case Study. *Atmos. Chem. Phys.* 18 (22), 16345–16361. doi:10.5194/acp-18-16345-2018

Conflict of Interest: The authors declare that the research was conducted in the absence of any commercial or financial relationships that could be construed as a potential conflict of interest.

Publisher's Note: All claims expressed in this article are solely those of the authors and do not necessarily represent those of their affiliated organizations, or those of the publisher, the editors and the reviewers. Any product that may be evaluated in this article, or claim that may be made by its manufacturer, is not guaranteed or endorsed by the publisher.

Copyright © 2021 Wu, Liu, Zhao, Su, and Zhou. This is an open-access article distributed under the terms of the Creative Commons Attribution License (CC BY). The use, distribution or reproduction in other forums is permitted, provided the original author(s) and the copyright owner(s) are credited and that the original publication in this journal is cited, in accordance with accepted academic practice. No use, distribution or reproduction is permitted which does not comply with these terms.